Metal−Support Interactions in Co/Al_2O_3 Catalysts: A Comparative Study on Reactivity of Support

L. Ji,[†,‡] J. Lin,[†] and H. C. Zeng[‡,*]

Department of Physics, Faculty of Science, and Department of Chemical and Environmental Engineering, Faculty of Engineering, National University of Singapore, 10 Kent Ridge Crescent, Singapore 119260

Received: September 22, 1999

Co/Al_2O_3 catalysts have been prepared with conventional impregnation and sol−gel methods to vary the chemical reactivity of the alumina support. The material system has been investigated with X-ray diffraction (XRD), Fourier transform infrared spectroscopy (FTIR), diffuse reflectance Fourier transform spectroscopy (DRIFT), Brunauer−Emmett−Teller (BET) method, X-ray photoelectron spectroscopy (XPS), temperature-programmed reduction (TPR) (with thermogravimetric analysis (TGA) and differential thermal analysis (DTA)), and gas chromotography (GC) for the catalytic oxidation of CO. It had been found that the reactivity of the support changes the surface structure and chemical composition of catalysts significantly. When the metal−support interaction is weak, Co_3O_4 is a predominant surface phase (which is interfaced by a "cobalt surface phase"). With an increase in support reactivity, CoO and $CoAl_2O_4$ are found to be present on the surface. The cobalt content on the surface decreases upon the increase in support reactivity and surface area. At the high atomic ratio of Al/Co, there are more ═Al−O−H bonds that show higher basicity. Reducibility of the phases observed decreases on the order of Co_3O_4, CoO, and $CoAl_2O_4$. It is found that the removal of CO on metallic sites is much easier in the catalyst with lower metal−support interactions. At room temperature, reactions between the adsorbed CO and lattice oxygen have been observed in all samples. The catalytic activity for the CO combustion reaction increases with the decrease in metal−support interactions of the catalysts. Possible causes for the above observations have been addressed.

Introduction

Cobalt catalysts supported on alumina are an important material system in the field of heterogeneous catalysis for the hydrogenation, hydrotreating, and combustion processes.[1−6] It has been reported that metal−support interactions may appreciably affect the surface properties, and hence catalytic reactivities. From the fundamental viewpoint, these interactions depend primarily upon factors such as the concentration of metal species, nature of the support, and temperature and duration of calcination, which in turn depends on the actual material selection and preparation method.[4,6,7] Surface active phases, for example, can be significantly differentiated via various preparative routes, even keeping the overall chemical composition constant for a catalyst.

Conventionally, supported Co/Al_2O_3 catalysts have been prepared by the impregnation method in an aqueous solution of cobalt salt using a commercial alumina support (in most cases, γ-Al_2O_3). The alumina support used, whose role is mainly as a dispersion medium, has been commonly heat-treated and shaped prior to impregnation and is generally expected not to be involved in formation of catalytically active components under normal processing conditions (300−500 °C). In other words, the metal−support interactions in such cases may not be fully appreciated or recognized.

It has been noted that, for the past decade, nanosized alumina with a large surface area has been prepared via various sol−gel routes at relatively low temperatures.[8−14] These sol−gel-derived materials would therefore represent a class of active "support"; they may participate positively or negatively in forming final catalysts. Using alumina xerogel as a support for impregnation, for example, the metal−support interactions can be significantly amplified, since this "raw" support could actively interact with impregnated metal when it transforms into final alumina upon heat treatment. In addition to the gain in chemical reactivity of support along the vertical direction of metal−support interface, extra dimensions for metal−support interactions can also be obtained by direct inclusion of metal species to the alumina xerogel matrix during the sol−gel synthesis. In such an extreme case, an included nanosized metal particle can interact with the matrix material in all directions (360°), i.e., with a curved interface instead of a flat one.

The present work reports a first comparative study of Co/Al_2O_3 catalysts with increasing chemical reactivity of the alumina support while keeping the weight of cobalt constant. To quantify metal−support interactions, chemical and physical properties of the prepared catalysts have been investigated with a wide variety of techniques such as X-ray diffraction (XRD), Fourier transform infrared spectroscopy (FTIR), diffuse reflectance Fourier transform spectroscopy (DRIFT), Brunauer−Emmett−Teller (BET) method, X-ray photoelectron spectroscopy (XPS), temperature-programmed reduction (TPR) (with thermogravimetric analysis (TGA) and differential thermal analysis (DTA)), and gas chromotography (GC) for the probe reaction of CO catalytic oxidation.

* To whom correspondence should be addressed. Tel: +65 874 2896. Telefax: +65 779 1936. E-mail: chezhc@nus.edu.sg.

[†] Department of Physics, Faculty of Science.

[‡] Department of Chemical and Environmental Engineering, Faculty of Engineering.

10.1021/jp993400l CCC: $19.00
Published on Web 02/04/2000

Experimental Section

Sample Preparation. Three Co/Al_2O_3 samples with 10 wt % in metal Co were prepared by different synthetic methods. Samples IM1 and IM2 were obtained by impregnation with different types of supports. Briefly, a certain amount of alumina support was soaked in a solution of cobaltous nitrate hexahydrate (Merck, >99%) in a predetermined amount of H_2O and was allowed to stand at room temperature overnight with frequent stirring. This was then followed with a drying at 120 °C for 3 h. Commercial γ-Al_2O_3 support (Merck) and sol−gel-derived dried alumina gel (which will described shortly) were used in IM1 and IM2, respectively. Sample SG was prepared by a sol−gel method using cobaltous nitrate hexahydrate and aluminum tri-*sec*-butoxide (ASB, ACROS, 97%) as precursor materials. In a typical synthesis, 5 mL of ASB was dissolved in the solution of 23 mL of 2-propanol (Fisher Scientific, >99.9%) and 0.5 mL of chelating agent acetylacetone (Merck, >99.5%) under a nitrogen atmosphere. This chelated precursor system was stirred vigorously at room temperature for 30 min. The cobaltous nitrate dissolved in 2 mL of deionzed water was added drop by drop under mild stirring for 30 min with a molar ratio of H_2O/Al (or ASB) equal to 6. The sample gelled in a few minutes, resulting in transparent pink gels. The resulting wet gels were aged at room temperature with cover for 5 days and then dried in an electric oven at 60 °C for 5 days. When only 2 mL of pure water (without cobaltous nitrate) was added, sol−gel-derived alumina gel could be obtained, which was used as the support in IM2 after drying. The above three samples were calcined at 400 °C for 2 h in static air, after which they were used as catalysts for property characterization and $CO + {}^1/_2O_2$ oxidation experiments.

Characterization Techniques. *XRD Measurement.* Structural phases were determined for crushed catalysts in a Shimadzu X-ray diffractometer using Cu Kα radiation. A continuous scan mode was used to collect 2θ data from 10° to 80° with a 0.02 sampling pitch and a 4°/min scan rate. X-ray tube voltage and current were set at 40 kV and 30 mA, respectively.

FTIR Measurement. The catalyst samples were characterized by FTIR spectroscopy in a Perkin-Elmer spectrometer (model 2000), using the potassium bromide (KBr) pellet technique. Thirty-two scans with a resolution of 4 cm^{-1} were performed for each spectrum.

BET Measurement. A NOVA 2000 was used to determine the specific surface area of the catalytic samples prepared. Before the measurements, the samples were degassed for 3 h at 350 °C in an outgassing station of the adsorption apparatus. The full adsorption−description isotherm was obtained at 77 K using the Brunauer−Emmett−Teller (BET) method at various relative pressures (6 points in the region of $0.05 < P/P° < 0.30$; nitrogen molecular cross-sectional area = 16.2 Å^2).

TPR Measurement. Reduction of the catalysts by H_2 was monitored by means of temperature-programmed reduction (TPR) in a Perkin-Elmer TGA instrument. Fifteen milligrams of catalyst powder was placed in a sample holder and heated from 100 to 900 °C at a rate of 10 °C/min in H_2 stream (flow rate = 22.7 mL/min), while the weight change was recorded as a function of temperature. Reduction of the catalysts by CO was also studied by means of TPR in a Perkin-Elmer DTA instrument. Thirty-five milligrams of sample was used and heated from 30 to 900 °C at a rate of 10 °C/min in CO stream (flow rate = 22.7 mL/min), while heat flux changes were recorded as a function of temperature.

CO Adsorption/Removal Measurement. In situ diffuse reflectance infrared Fourier transform (DRIFT) studies on CO adsorption/removal were performed in the Perkin-Elmer 2000 equipped with a reaction cell as well as the DRIFT accessory (Harrick). The catalyst was loaded in the reaction cup inside the reaction cell and was purged with He (flow rate = 30 mL/min) at 350 °C for 1 h before the reaction. The CO gas was then introduced to the reaction cell at a speed of 30 mL/min, keeping in contact with the examined catalyst. After the adsorption, the CO-removal experiment was immediately commenced with purging gas He again at 30 mL/min. The DRIFT spectra were recorded from 400 to 4000 cm^{-1} with a resolution of 8 cm^{-1}. One hundred scans were made for each spectrum to ensure a good signal-to-noise ratio.

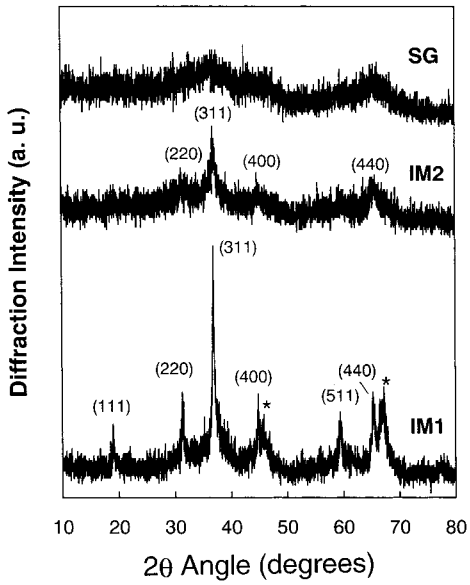

Figure 1. XRD patterns for the as-prepared catalysts (calcined in static air at 400 °C for 2 h). The asterisk (*) indicates the γ-Al_2O_4 phase from the support.

XPS Measurement. XPS investigation was conducted on a VG ESCALAB-MKII spectrometer using an Al Kα X-ray source (1486.8 eV, 120 W) at the constant analyzer pass energy of 20.0 eV. All binding energies (BE) were referenced to the C 1s peak (BE = 284.5 eV) arising from adventitious carbon. Prior to the curve fitting, X-ray satellites and inelastic background (linear-type) were subtracted in all cases, and 80% Gaussian and 20% Lorentzian peaks were used in the peak deconvolution.

Catalytic Activity Measurement. The CO oxidation tests were carried out in a tubular flow reactor controlled by a Ycc-16 computer-programmed controller at atmospheric pressure. About 200 mg of catalyst was pretreated in a gas mixture of $Ar:O_2$ (90%:10%) at 350 °C for 1 h. A gas stream of 8 mL/min CO and 4 mL/min O_2, which was balanced with He to a total flow rate of 50 mL/min, was continuously passed through the catalyst bed. The effluent from the reactor was analyzed by gas chromatography (GC, Shanghai FXYQC, 102G-D) with a thermal conductivity detector. A molecular sieve 5A column (Supelco) was used for the separation of reactants and products. The $CO + {}^1/_2O_2$ combustion reaction was studied at various temperatures between 100 and 450 °C.

Results

Catalyst Structure. XRD patterns of the three as-prepared catalysts (which were calcined at 400 °C for 2 h) are shown in Figure 1. As can be seen, the pattern of IM1 has relatively high diffraction intensities of the cubic spinel phase such as Co_3O_4 and/or $CoAl_2O_4$ and γ-Al_2O_3 phase.[4−6] The IM2 sample has

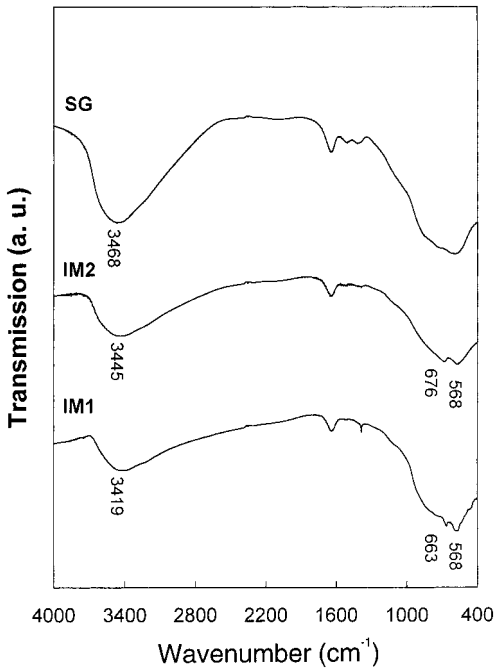

Figure 2. FTIR spectra for the as-prepared catalysts.

the same spinel diffraction pattern as IM1, but with much lower intensities, and no γ-Al_2O_3 phase can be detected. The XRD peak breadth for the SG sample is even broader, which reveals a nanosized crystalline state in this sample. It is difficult to establish the chemical and structural phases for the three samples based on XRD characteristics alone because Co_3O_4 and $CoAl_2O_4$ both have cubic spinel structure with almost identical diffraction peak positions.[4−6] Nonetheless, the difficulty in resolving these two phases can be overcome by FTIR and XPS techniques.

Figure 2 shows the FTIR spectra of the three as-prepared catalysts. A band at 3419 cm^{-1} in the IM1 sample can be assigned to the stretching vibration of hydroxyl groups O−H. Within the region of 700−500 cm^{-1}, strong doublet peaks at 663 and 568 cm^{-1} are typical metal−oxygen vibrations in the cubic spinel oxide of Co_3O_4 as reported in the literature.[15] The IR spectrum of IM2 is quite similar to that of IM1 but with shifts in the O−H and metal−oxygen stretching bands toward higher wavenumber regions (at 3445 and 676 cm^{-1}, respectively). In particular, the 676 and 568 cm^{-1} doublet peaks correspond to the literature data for the $CoAl_2O_4$ phase (675 and 567 cm^{-1}),[5] noting that, in good agreement with the XRD results, they are not as intense as those of IM1. In the sample SG, the O−H stretching band is shifted even more (to 3468 cm^{-1}) and with much higher intensity, whereas only a weak spinel doublet feature (also assigned to $CoAl_2O_4$ phase) can be observed. The water bending mode is observed in all samples (ca. 1630 cm^{-1}), while the trace NO_3^- (1385 cm^{-1}) and CO_3^{2-} (1430−1410 cm^{-1}) can be detected in IM1 and SG, respectively.[1]

Surface Analysis of Catalysts. The BET specific surface area (S_{BET}) measurement reveals that among the three samples, SG (which was prepared via the sol−gel method) has the highest surface area of 211 m^2/g, while IM1 has the smallest value of 120 m^2/g. The IM2 sample has a high S_{BET} of 197 m^2/g, because its alumina support was also sol−gel derived.

Figure 3 displays the Co 2p photoelectron spectra recorded for the three as-prepared samples. XPS analytical results on Co $2p_{3/2}$ binding energies are presented in Table 1, followed by the literature data of various Co-containing compounds in Table 2.[16] As can be seen, the Co $2p_{3/2}$ component at 779.3 eV

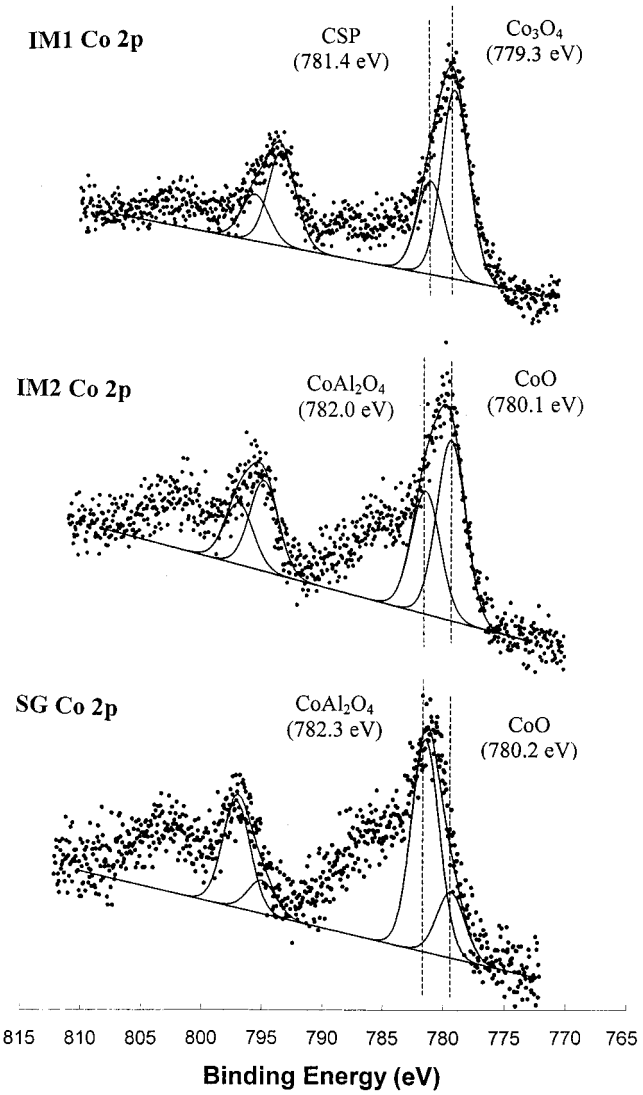

Figure 3. XPS spectra of Co 2p for the as-prepared catalysts.

TABLE 1: Cobalt $2p_{3/2}$ Binding Energy (BE), Spin−Orbit Coupling (SOC), and Atomic Ratios of Al/Co and Al/C for the As-Prepared Samples

sample	BE (eV) 1st peak	SOC (eV)	BE (eV) 2nd peak	SOC (eV)	Al/Co	Al/C
IM1	779.3	14.9	781.4	15.1	3.26	2.15
IM2	780.0	15.6	782.0	15.5	3.75	1.05
SG	780.2	15.5	782.3	15.6	5.22	1.16

TABLE 2: XPS Data and Characteristics of Cobalt-Containing Reference Materials[4]

material	Co $2p_{3/2}$ BE (eV)	reliability (eV)	shake-up satellite	spin−orbit coupling (eV)
Co	778.1	±0.1		15.1
CoO	780.1	±0.9	strong	15.5
Co_3O_4	780.0	±0.7	weak	15.0
$Co(OH)_2$	780.9	±0.2	strong	16.0
$Co(NO_3)_2$	781.9		strong	16.0
$CoAl_2O_4$	781.9	±0.5	strong	15.5

indicates that the surface cobalt is largely present as Co_3O_4 in the IM1 sample. The other component at 781.4 eV cannot be assigned to bulk $CoAl_2O_4$ because there is no shake-up satellite observed (Table 2) and low reactivity in the commercial γ-Al_2O_3 support is generally expected. Nevertheless, this component can be attributed to a cobalt surface phase (CSP), as assigned in the catalyst system using a similar impregnation method with a

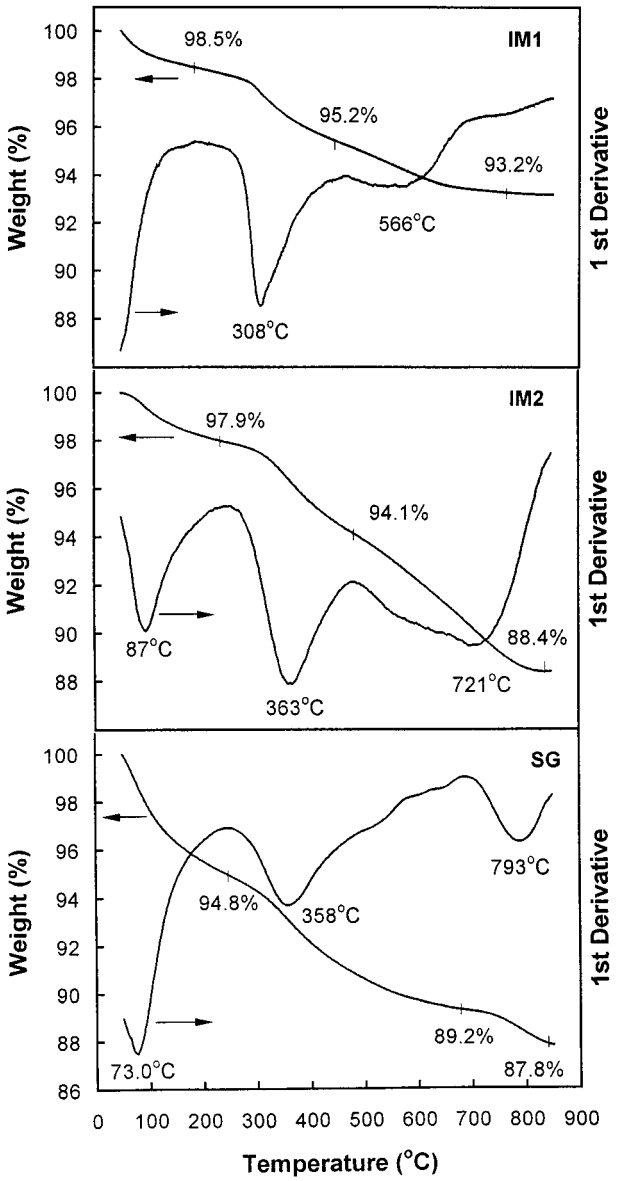

Figure 4. H_2-TPR investigation for the as-prepared catalysts using TGA method. H_2 flow rate: 22.7 mL/min.

commercial γ-Al_2O_3 support.[16−18] It is noted that the cobalt nitrate precursor ($Co(NO_3)_2 \cdot 6H_2O$) thermally decomposes to Co_3O_4 oxides at around 300 °C.[3] The CSP phase was believed to cover over the alumina support during the calcination and it is a hardly reducible surface phase.[16−18] In the absence of solid-state diffusion into the support matrix, this surface phase is highly dispersed and is presumably present in the monolayer thickness.[16−18]

For the IM2, the Co $2p_{3/2}$ peaks are accompanied by strong shake-up satellites. The peak at BE = 780.0 eV is the characteristic of cobalt monoxide CoO, because CoO, rather than Co_3O_4, has a strong shake-up satellite peak 5 eV higher than its main peak and has a spin−orbit coupling of around 15.5 eV (Tables 1 and 2).[2,16] Another peak at BE = 782.0 eV is assigned to $CoAl_2O_4$, since $CoAl_2O_4$ also has a strong shake-up satellite at the energy 6 eV higher.[16]

Similar to the IM2 sample, CoO is a surface component in the SG sample with its Co $2p_{3/2}$ peak at 780.2 eV but with a much lower intensity, which indicates a strong interaction between the cobalt oxide and alumina.[2,7,16] For a similar reason, the second peak at 782.3 eV cannot be assigned to CSP but to

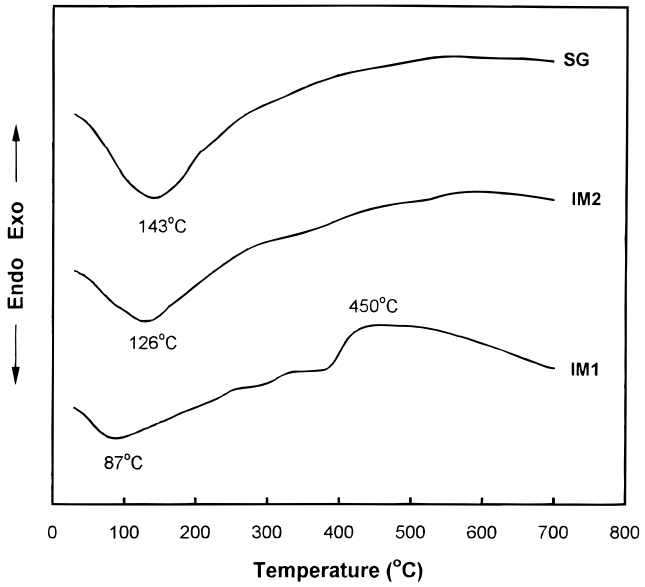

Figure 5. CO-TPR investigation for the as-prepared catalysts using DTA method. CO flow rate: 22.7 mL/min.

$CoAl_2O_4$, since stronger satellites for both CoO and $CoAl_2O_4$ are also observed in this sample.[16]

Chemical Reactivity of Catalysts. H_2-TPR (TGA) results for the three catalyst samples are presented in Figure 4. The low-temperature weight losses can be assigned to a de-moisture process, since they complete largely before 100 °C. On the basis of the XRD/FTIR results in Figures 1 and 2, it is known that $Co(NO_3)_2 \cdot 6H_2O$ had been completely decomposed during the catalyst preparation (400 °C) in all three samples. The IM1 sample has a sharp weight loss at 308 °C and a shoulder at higher temperature (asymmetrical peak with a total loss of 3.3%), which can be assigned to reductions of Co_3O_4 and CoO (resulted from in-situ reduction of Co_3O_4[2]), respectively.[3,4] The second band at 566 °C with a weight loss of 2.0% can be attributed to the CSP reduction process. In IM2 and SG samples, a symmetrical peak observed at 363 °C (IM2) and 358 °C (SG) can be assigned unambiguously to the reduction of the CoO phase, while the high-temperature losses at 721 and 793 °C are assigned to the reduction of $CoAl_2O_4$.[3,4] The symmetrical peaks observed at 363 and 358 °C indicate that there is no Co_3O_4 phase in IM2 and SG. It is known that, on the basis of these H_2-TPR results, both IM2 and SG samples are more difficult to reduce compared to IM1.

The above finding is further confirmed by the CO-TPR (DTA) investigation, which is shown in Figure 5. Once again, the sample IM1 shows the lowest reduction temperature among the three, while the completion of the $CoAl_2O_4$ reduction becomes difficult to define except for the case of IM1 at 430−450 °C, which has been attributed to the reduction of CSP.

The investigation on adsorption and desorption of carbon monoxide also reveals the significant difference between the Co_3O_4-containing sample (IM1) and CoO-containing samples (IM2 and SG). As shown in IR spectra of Figure 6, two large absorption bands at 2172 and 2117 cm^{-1} can be observed immediately after the CO gas was introduced. The band of 2172 cm^{-1} lies at a higher frequency than that of gaseous CO (2143 cm^{-1}),[15,19] which suggests the CO molecule is absorbed in a relatively high oxidation state cation through donating its electrons in this σ-type coordination bond.[15,19] The band can be therefore be assigned to the CO adsorption in the coordinatively unsaturated Co^{3+} sites. The band centered at 2117 cm^{-1}, as reported previously in many cases in the literature,[5,15,19,20]

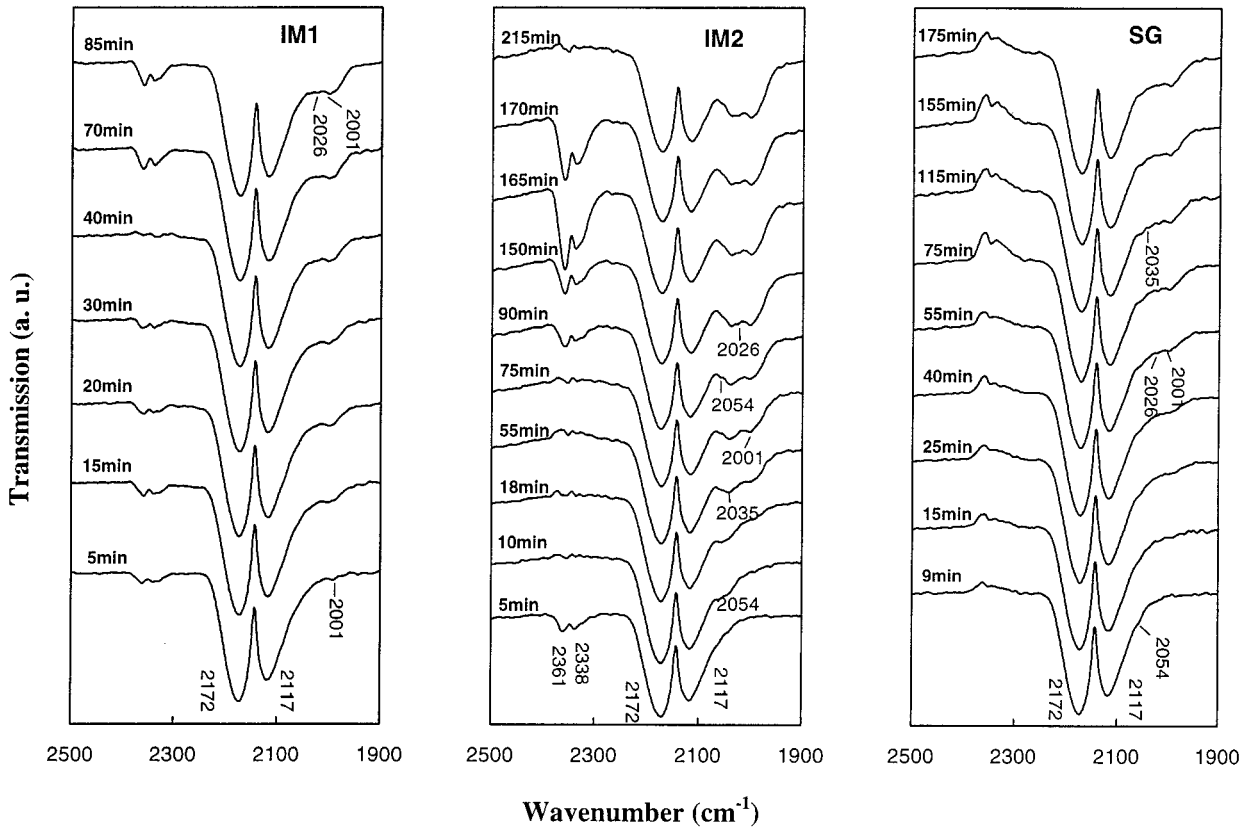

Figure 6. In situ DRIFT study of CO adsorption on the as-prepared catalysts. CO flow rate: 30 mL/min.

can be ascribed to the CO on Co^{2+} sites. These assignments are also in line with the fact that Co_3O_4 is a predominant surface phase in the IM1 sample.

In addition to the CO on cationic sites, the adsorption of CO at room temperature also gives an IR stretching peak of C−O at 2001 cm^{-1} and a high-frequency shoulder at 2026 cm^{-1} after 70 min of experiment (Figure 6). According to the literature data,[5,15,19,20] both absorptions can be assigned to CO linearly ligated to zerovalent Co^0 sites (or more reduced sites). The high-frequency shoulder at 2026 cm^{-1} may be attributable to CO adsorption at higher coverage, as it appears only at a later stage of the adsorption in this sample. Emergence of 2001 and 2026 cm^{-1} peaks indicates the presence of metallic cobalt, which is reduced from high oxidation state cations upon CO adsorption.

Similar to IM1, IM2 and SG samples also have the high-oxidation-state IR absorptions at 2172 and 2117 cm^{-1}, which can be assigned accordingly to trivalent and divalent cations, Al^{3+} (octahedrally coordinated Al^{3+} exposed ions) and Co^{2+}, respectively.[15,20] Unlike IM1, however, a small band at the low frequency side of 2054−2035 cm^{-1} appears within 10 min of CO adsorption. According to the literature, this band can be assigned to multicarbonyl ligation to Co^+ (or $Co^{\delta+}$), which show fewer electron-donor properties, or Co^0 sites.[5,15,19,20] The band at 2001 cm^{-1} is also quite large in IM2, compared to those IR spectra with similar CO exposure times (85 min in IM1 and 90 min in IM2). Overall IR absorptions at 2054−2001 cm^{-1} for the SG sample are very similar to those of IM2 except with much smaller intensities. For example, the 2054 cm^{-1} peak also appears earlier than the 2001 cm^{-1} in both cases.

In Figure 7, the removal of adsorbed CO in all three samples is presented. In all cases, the intensities of cationic CO vibration peaks (2172 and 2117 cm^{-1})[5,15,19,20] are reduced significantly upon the helium purging. A great difference observed between IM1 and IM2 is that CO adsorbed on cationic sites and metallic cobalt sites (2026−2001 cm^{-1})[5,15,19,20] is removed simultaneously in IM1 while the CO on cationic sites disappears much earlier than on the metallic sites (2054−2001 cm^{-1}) in IM2. This is also true for the SG sample, which shows a similar early removal of the metallic site adsorption at 2054−2001 cm^{-1}. On the basis of these dynamic data, it is indicated that the removal of CO from the IM1 surface is much easier than from IM2.

Figure 8 shows the CO oxidative conversion to CO_2 on the three different catalysts as a function of reaction temperature. The IM1 sample has the highest reaction activity with 100% conversion at 170 °C, while IM2 is able to convert CO totally to CO_2 at 230 °C. The SG sample shows the lowest activity with 100% conversion at as high as 425 °C.

As also revealed in both Figures 6 and 7, CO adsorption and CO removal on catalyst surfaces at room temperature show some remarkable effects on the CO_2 IR intensities at 2361 and 2338 cm^{-1}.[1,21] The observed oscillation in IR peak intensities indicates a complex CO adsorption and its reaction with lattice oxygen, which will be addressed further in the next section.

Discussion

Chemical Reactivity between the Support and Catalysts. It is known that the interaction between the catalyst and its support affects the surface properties and thus overall catalytic activity. In the present work, the degree of metal−support interactions has been varied by the different preparative methods.

Among the three catalysts, the support for IM1 is the least active in terms of the metal−support interaction. Because of its small surface area (121 m^2/g), it is understood that thicker cobalt oxides will be deposited on the surface and the least catalyst−support interaction for this catalyst is expected. This is evidenced in XRD, FTIR, and XPS results that Co_3O_4 is a

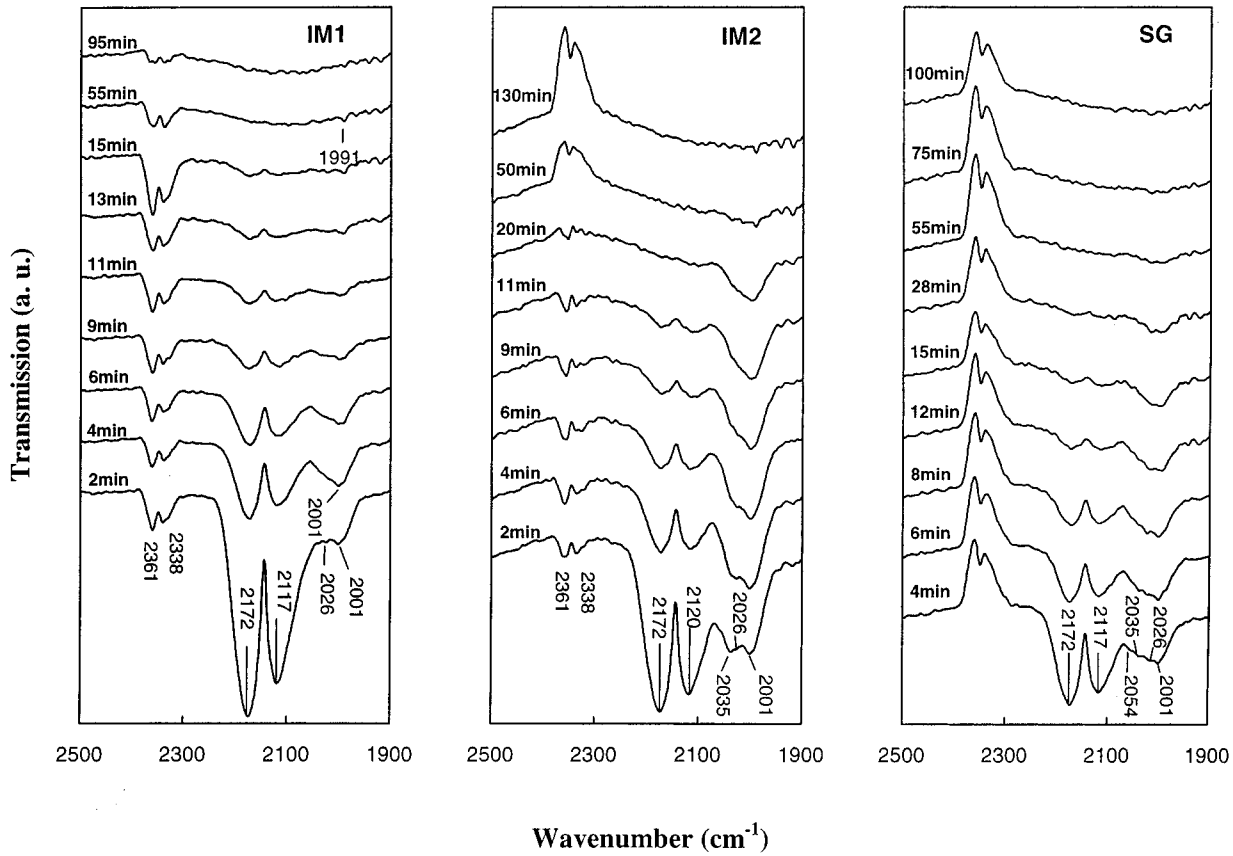

Figure 7. In situ DRIFT study on CO removal (direct He purging and formation of CO_2) for the as-prepared catalysts. He flow rate: 30 mL/min.

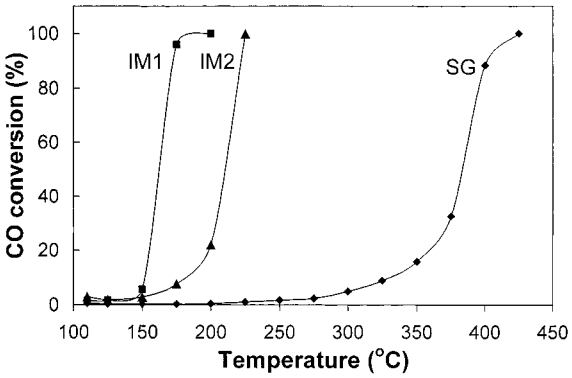

Figure 8. Activity evaluation for the CO + $^1/_2O_2$ reaction on the as-prepared catalysts. CO flow rate: 8 mL/min. O_2 flow rate: 4 mL/min.

dominant phase in the IM1 sample, in which γ-Al_2O_3 acts only as a dispersion medium. The observed Co_3O_4 phase was formed from the decomposition of $Co(NO_3)_2{\cdot}6H_2O$, which was introduced to the γ-Al_2O_3 support through impregnation. It should be mentioned that since the commercial γ-Al_2O_3 we used is chemically more stable, it is hard for cobalt ions to penetrate into the support matrix to form bulk $CoAl_2O_4$ spinel at 400 °C, compared to the in situ prepared γ-Al_2O_3 support in the IM2 case. As for the SG sample, cobalt ions (in the form of $Co(NO_3)_2{\cdot}6H_2O$) have been premixed in the alumina gel matrix and the $CoAl_2O_4$ phase can be readily formed, as revealed by the XPS surface analysis. The easy formation of the spinel phase $CoAl_2O_4$ indicates a stronger interaction of cobalt and alumina gel in the SG sample due to good dispersion of $Co(NO_3)_2{\cdot}6H_2O$. It should be mentioned that the $CoAl_2O_4$ phase formed in the SG sample is in nanometric scale, judging from the XRD pattern (Figure 1) and ill-defined bands in the FTIR spectrum (Figure 2). Because of the possibility of Al−O−Co formation during the gelation (no XRD pattern of $Co(NO_3)_2{\cdot}6H_2O$ can be detected for the xerogel of SG sample), it is understandable that the aluminum and cobalt could have a better mixing at the atomic level that leads to the formation of the $CoAl_2O_4$ phase. Of course, not all $Co(NO_3)_2{\cdot}6H_2O$ are reacted. The unreacted $Co(NO_3)_2{\cdot}6H_2O$ would simply be converted to cobalt oxide when heat-treated later.

Compared with the SG sample, the metal−support interaction in IM2 was not present until cobalt was impregnated into the xerogel of alumina, especially when calcination of the impregnated gel was conducted. When an alumina xerogel of this type was transformed to a metal oxide, it is known that the old chemical bonds will be broken and new ones will be formed.[22] In other words, aluminum cations will be more active during this transforming process. When thermally decomposed, the $Co(NO_3)_2{\cdot}6H_2O$ gives away CoO, which will then react with the xerogel-derived alumina support. Similar to the SG sample, this process allows the formation of the $CoAl_2O_4$ phase from newly born CoO and Al_2O_3. Unlike the SG sample, however, the spinel formation in IM2 will be mainly in the interfacial region between the impregnated $Co(NO_3)_2{\cdot}6H_2O$ and support of alumina xerogel.

It is noted that the IR spectra in the ν(O−H) region of 3419−3468 cm^{-1} can all be assigned to the hydrogen-bonded hydroxyl groups.[20] Since the XPS study does not suggest the existence of $Co(OH)_2$, the observed hydroxyl groups should be assigned only to ═Al−OH. Although the hydroxyl groups in SG are the most abundant among the three studied samples, SG's basicity is the highest (with a high wavenumber at 3468 cm^{-1}, Figure 2), i.e., less hydrogen bonding or less perturbed.[20] The abundance of ═Al−OH can be attributed to incomplete condensation reactions,[22] while the higher basicity observed can be attributed to a replacement of Co^{2+} for Al^{3+} in the Co−O−Al linkage in

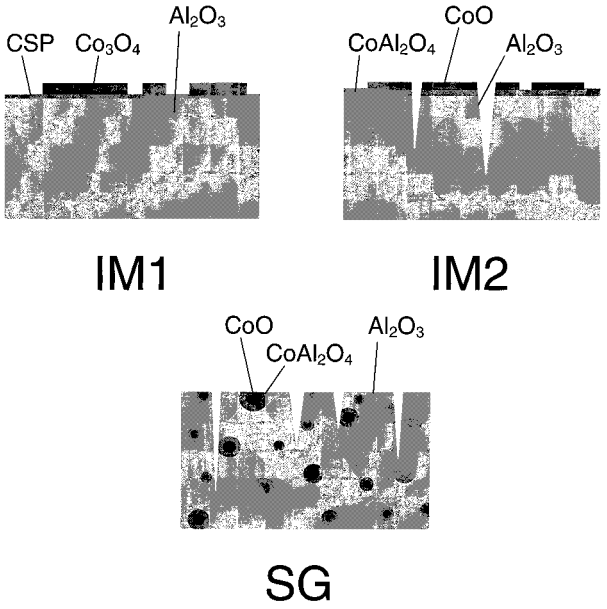

Figure 9. Deduced surface models for the three catalysts, noting that the drawing representation does not follow the actual scale of each catalyst.

the alumina matrix, as Co^{2+} has less polarization power than Al^{3+}. Furthermore, more surface species of ═Al−OH are expected in the SG catalyst since it was prepared using the nonimpregnation method.

Structures and Surface Compositions of the Catalysts. On the basis of the above XRD/FTIR/XPS analyses, structures for the three catalysts can be summarized schematically in Figure 9. For the cobalt oxide system, it has been known that the Co_3O_4 is a thermodynamically stable surface phase under the ambient condition while the CoO phase is only stable at temperatures of 1000−2000 °C. The transition between the two oxides can be expressed as

$$Co_3O_4 \leftrightarrow 3CoO + {}^1/_2O_2 \qquad (1)$$

in which the reverse reaction is exothermic because of oxidation of divalent cobalt.[23] This is true for the IM1 catalyst, since only Co_3O_4 phase is observed by XPS on the surface at room temperature. It has been known that the extra stability of divalent cobalt oxide can be obtained by using the oxide supports, which has been illustrated recently in the catalyst systems of CoO/ZrO_2 and CoO/MgO.[24,25] As analyzed in the previous subsection, the catalyst−support interaction is stronger in IM2 and the formation of $CoAl_2O_4$ in the alumina gel has lessened the cobalt oxide on the surface. Because of the thinner cobalt oxide layer on the surface, CoO becomes a stable phase. The support of $CoAl_2O_4$ in such a case is thus believed to be able to keep surface CoO from further oxidation.[24] A similar explanation on the stabilizing effect of support can be extended to the SG sample surface, on which CoO is the only cobalt oxide species. It should be mentioned that, according to the XPS analysis (Figure 3) and the model in Figure 9, the surface CoO phase of SG should exist only in a small quantity. It seems that the nanometrical size of the CoO particles encapsulated in the shells of the $CoAl_2O_4$ support has an effect similar to that of the thin surface layer on the phase stability.

In agreement with the above surface analyses, the surface atomic ratio of Al to Co increases from 3.26 to 5.22 in the three studied samples (Table 1). For the impregnated samples, in principle, they should have a lower Al/Co ratio because Co was coated only on the external surfaces that include pore surfaces. It should be noted that the alumina support in IM1 did not suffer severe thermal deformation, as it is more stable than that in IM2. Because of the chemical reactions and cracking of the alumina xerogel during the calcination, some naked area (without Co coating) of the gel support may be generated (IM2, Figure 9), which results in a higher Al/Co ratio in IM2 (3.75). In contrast to IM1 and IM2, aluminum is a predominant surface species in the SG sample (Figure 9), as alumina is the matrix material while CoO and $CoAl_2O_4$ are imbedded subphases. Accordingly, the atomic ratio of Al/Co in SG is thus the highest among the three catalysts. On the basis of the XPS data (Table 1), it is noted that IM2 and SG have a lower atomic ratio of Al/C than IM1. In addition to the nature of the organically derived support and matrix (sol−gel method used in IM2 and SG) that contain more carbon species, the significant increase in carbon content can also be related to higher capacity in chemisorption of calcination product CO_2. As shown in Figure 2, the OH groups in these two samples (particularly in the SG sample) are more abundant and basic, which leads to more CO_2 (acidic) adsorption to form CO_3^{2-}. Clearly, by controlling the degree of catalyst−support interaction, the surface composition and catalyst structure can be engineered.

Reduction and Reaction Activities of Catalysts. Because of the structural difference, the reduction behaviors of the three catalysts are different. In Figure 4, the band at 566 °C is attributed to the reduction of CSP in the IM1 sample since the layer is thin (it was believed only to be one monolayer in thickness[16−18]). The band peaking at 721 °C in the IM2 sample is assigned to the reduction of $CoAl_2O_4$ after the CoO phase reduction (363 °C). It is interesting to note that the reduction of the $CoAl_2O_4$ phase in the SG sample is centered at a much higher temperature of 793 °C while the reduction of the CoO phase is at a lower temperature of 358 °C. Following the structural explanation in Figure 9, it is understandable that the reduction of the CoO phase is largely completed prior to that of the $CoAl_2O_4$ phase in the IM2 sample while some CoO (bulk phase) in SG has to be reduced only after the reduction of $CoAl_2O_4$. Because of the nanosized surface CoO phase in SG, the reduction is relatively easier (i.e., the temperature is lower at 358 °C). However, for the bulk phase CoO, which is encapsulated in the shells of $CoAl_2O_4$, the reduction of CoO will be delayed. Because of the nature of the composite structure (Al_2O_3 matrix + $CoAl_2O_4$ (which includes CoO), Figure 9), the reduction of the $CoAl_2O_4$ phase becomes difficult (i.e., the temperature is higher). In this regard, the reductions at 358 °C (and its shoulders) should be assigned to the CoO and then $CoAl_2O_4$ while the reductions at 793 °C should be attributed to the $CoAl_2O_4$ and then CoO.

Comparing Figure 5 with Figure 4, we recognize that the reduction of Co-containing oxides in CO is less informative, since only one endothermic effect is shown in the early stage of the reduction (at 87, 126, and 143 °C for IM1, IM2, and SG, respectively). More specifically, with CO gas (instead of H_2), the reductions between Co_3O_4 and CoO in the sample IM1 are not distinguishable. A completion point at 450 °C for the IM1 sample can be observed, whereas no such turning is observed for IM2 and SG within the studied temperature range, which indicates that the reduction with CO gas is a long-lasting process.

Upon the reduction of the above catalysts with CO at room temperature, the oscillation profiles for the product compound CO_2 (2361 and 2338 cm^{-1}) have been shown in both Figures 6 and 7. In Figure 6, with an increase in CO exposure time, both CO adsorbed in metallic sites (2026−2001 cm^{-1} in IM1 and

2054−2001 cm^{-1} in IM2) and CO_2 formation can be observed at the same time, which is more apparent in IM2. It seems that even at room temperature an adsorbed CO can be oxidized into molecular CO_2 by the cobalt cations in combination with a surface oxygen:

$$CO_{(ad)} + O^{2-}Co^{2+} \rightarrow CO_{2(ad)} + Co^{0} \quad (2)$$

In a He purging experiment (Figure 7), there is no supply of gas phase CO and the removal of adsorbed CO can be largely divided into two parts, direct purging (desorption) and oxidative conversion to CO_2. As reported in the Results (Figure 7), a great difference between IM1 and IM2 is that CO adsorbed on cationic sites (2172−2117 cm^{-1}) and metallic cobalt sites (2026−2001 cm^{-1})[5,15,19,20] are removed simultaneously in IM1 while the CO on cationic sites disappear much earlier than on the metallic sites (2054−2001 cm^{-1}) in IM2. The difference indicates a synchronized removal of the adsorbed CO on both cationic and metallic sites in the IM1 sample, apart from the direct removal of CO by an He purge. As the gain in CO_2 signal in IM1 is large upon the removal of CO from the metallic sites, it is believed that CO can be driven from a metallic site to cationic sites on which reaction 2 takes place, noting that the Co^{3+} is present only in IM1. In the absence of oxygen, the oxidative formation of CO_2 leads to the following two reactions, which will eventually eliminate the surface cationic sites:

$$Co^{3+} + e^{-} \rightarrow Co^{2+} \quad (3)$$

$$Co^{2+} + 2e^{-} \rightarrow Co^{0} \quad (4)$$

Interestingly, unlike in IM1, both CO bands and CO_2 bands in IM2 are reduced gradually and, eventually, the CO_2 bands become reversed after 20 min of He purging, when CO bands (on metallic sites) are not detectable. This band reversion seems to indicate weaker chemical activity of IM2 to CO oxidation, as less CO_2 are formed during the He purging due to lack of cationic adsorption sites (note that there is no trivalent Co^{3+} in this sample). The adsorption and removal of CO in the SG sample are quite similar to those of IM2. In fact, the reversion in CO_2 bands takes place from the beginnings of the both processes (Figures 6 and 7). However, within each series of IR spectra, a small variation in negatives can still be noted, which seemingly suggests poor activity for CO_2 generation.

The above observations and explanations on chemical reactivity of the surface are in good agreement with the experimental results of CO catalytic oxidation in which O_2 was continuously supplied to the reaction. In the catalytic reactions reported in Figure 8, indeed, the IM1 has the highest catalytic activity for the reaction among the three catalysts, which is in good agreement with the fact that Co_3O_4 shows the highest catalytic activity for the combustion of CO among the binary cobalt oxides.[26] It has been proposed that the active oxygen species in selective oxidation generally comes from the lattice O^{2-} at the surface.[27,28] In such cases, cationic sites can be regenerated with the supply of oxygen, i.e., following the reverse reactions of (3) and (4), noting that the role of surface metal cations changes from an oxidant to a catalyst for the CO + $^1/_2O_2$ oxidation reaction.

Conclusions

In summary, with an increase in chemical reactivity of the alumina support, the surface structure and chemical composition of Co/Al_2O_3 catalysts can be controlled to meet a desired application. It has been found that Co_3O_4 is a predominant surface phase (which is interfaced by a "cobalt surface phase") when the metal−support interaction is small, and CoO and $CoAl_2O_4$ are surface phases as metal−support interactions increase. The surface content of cobalt reduces with respect to increases in chemical reactivity and surface area of the support. For the surfaces with a higher atomic ratio of Al/Co, ═Al−O−H bonds are more abundant and exhibit higher basicity. Reducibility of the spinel phase decreases according to the degree of metal−support interactions (Co_3O_4, CoO, then $CoAl_2O_4$). The CO adsorption takes place on both cationic and metallic sites in all studied samples. However, the removal of CO on metallic sites is much easier in the catalyst with lower metal−support interactions. Reactions between the adsorbed CO and lattice oxygen have been observed in all samples at room temperature. Catalytic activity for the CO combustion reaction (CO + $^1/_2O_2$) increases with a decrease in metal−support interactions of the catalysts. With variations in the support chemical reactivity, as shown in this work, the structure and chemical nature of Co/Al_2O_3 catalysts can be investigated in a greater depth.

Acknowledgment. We gratefully acknowledge research funding (RP960716 and A/C 50384) cosupported by the Ministry of Education and the National Science and Technology Board of Singapore. J.L. wishes to thank the National University of Singapore for providing postgraduate scholarship.

References and Notes

(1) Goodsel, A. J. *J. Catal.* **1973**, *30*, 175.
(2) Sexton, B. A.; Hughes, A. E.; Turney, T. W. *J. Catal.* **1986**, *97*, 390.
(3) Lapidus, A.; Krylova, A.; Kazanskii, V.; Borovkov, V.; Zaitsev, A. *Appl. Catal.* **1991**, *73*, 65.
(4) Wang, W.-J.; Chen, Y.-W. *Appl. Catal.* **1991**, *77*, 223.
(5) Busca, G.; Lorenzelli, V.; Bolis, V. *Mater., Chem. Phys.* **1992**, *31*, 221.
(6) Chokkaram, S.; Srinivasan, R.; Milburn, D. R.; Davis, B. H. *J. Mol. Catal. A* **1997**, *121*, 157.
(7) Chin, R. L.; Hercules, D. M. *J. Phys. Chem.* **1982**, *86*, 360.
(8) Babonneau, F.; Coury, L.; Livage, J. *J. Non-Cryst. Solids* **1990**, *121*, 153.
(9) Nass, R.; Schmidt, H. *J. Non-Cryst. Solids* **1990**, *121*, 329.
(10) Rezgui, S.; Gates, B. C. *Chem. Mater.* **1994**, *6*, 2386.
(11) Rezgui, S.; Gates, B. C.; Burkett, S. L.; Davis, M. E. *Chem. Mater.* **1994**, *6*, 2390.
(12) Tadanaga, K.; Ito, S.; Minami, T.; Tohge, N. *J. Non-Cryst. Solids* **1996**, *201*, 231.
(13) Vaudry, F.; Khodabandeh, S.; Davis, M. E. *Chem. Mater.* **1996**, *8*, 1451.
(14) Elaloui, E.; Pierre, A. C.; Pajonk, G. M. *J. Catal.* **1997**, *166*, 340.
(15) Busca, G.; Guidetti, R.; Lorenzelli, V. *J. Chem. Soc., Faraday Trans.* **1990**, *86*, 989.
(16) Zsoldos, Z.; Guczi, L. *J. Phys. Chem.* **1992**, *96*, 9393.
(17) Zsoldos, Z.; Hoffer, T.; Guczi, L. *J. Phys. Chem.* **1991**, *95*, 798.
(18) Guczi, L.; Hoffer, T.; Zsoldos, Z.; Zyade, S.; Maire, G.; Garin, F. *J. Phys. Chem.* **1991**, *95*, 802.
(19) Bailie, J. E.; Rochester, C. H.; Hatchings, G. J. *J. Chem. Soc., Faraday Trans.* **1993**, *13*, 2331.
(20) Busca, G.; Lorenzelli, V.; Escribano, V. S.; Guidetti, R. *J. Catal.* **1991**, *131*, 167.
(21) Finocchio, E.; Busca, G.; Lorenzelli, V.; Escribano, V. S. *J. Chem. Soc., Faraday Trans.* **1996**, *92*, 1587.
(22) Ji, L.; Lin, J.; Tan, K. L.; Zeng, H. C. *Chem. Mater.*, in press.
(23) Xu, Z. P.; Zeng, H. C. *J. Mater. Chem.* **1998**, *8*, 2499.
(24) Zeng, H. C.; Lin, J.; Tan, K. L. *J. Mater. Res.* **1995**, *10*, 3096.
(25) Drago, R. S.; Jurczyk, K.; Kob, N. *Appl. Catal. B* **1997**, *13*, 69.
(26) Boreskov, G. K. *Catalysis, Science and Technology*; Anderson, J. R., Boudart, M., Eds.; Springer: Berlin, 1982; Vol. 3, p 39.
(27) Satterfield, C. N. *Heterogeneous Catalysis in Industrial Practice*; McGraw-Hill: New York, 1991.
(28) Bielanski, A.; Haber, J. *Oxygen in Catalysis*; Dekker: New York, 1991.